

## Influence of Ion Energy on Carrier Activation and Source/Drain Parasitic Resistance in Low-Energy Ion Implantation for 0.15- $\mu\text{m}$ MOSFETs

Akio NISHIDA, Eiichi MURAKAMI, and Shin'ichiro KIMURA

*Central Research Laboratory, Hitachi Ltd.,*

*1-280 Higashi-Koigakubo, Kokubunji, Tokyo 185, Japan*

Low-energy ion implantation was investigated in detail as a method of forming shallow and low resistance source/drains (S/Ds) for 0.15- $\mu\text{m}$  MOSFETs. Rapid thermal annealing was found to be essential for obtaining diffused layers with low sheet resistance when the ion energy was decreased to 10 keV. Moreover, an increase in S/D edge resistance was observed in the fabricated MOSFETs. Thus, a relatively high implantation dose is necessary to obtain S/D diffused layers with low parasitic resistance.

### I. Introduction

The formation of an ultra-shallow diffused layer with a depth of less than 50 nm is essential for 0.15- $\mu\text{m}$  MOSFETs<sup>(1)-(2)</sup>. To obtain an ultra-shallow diffused layer by ion implantation, the ion energy should be lowered to reduce the ion projection range. The source/drain (S/D) parasitic resistance should also be lowered for high-performance operation. Thus, the electrical characteristics of ultra-shallow diffused layers need to be clarified. However, there have been no detail reports concerning ultra-shallow diffused layers fabricated by low-energy ion implantation. In this paper, we report on the influence of implantation energy on the carrier activation and sheet resistance, and on the S/D parasitic resistance of 0.15- $\mu\text{m}$  MOSFETs.

### II. Influence of Ion Energy on Carrier Activation and Sheet Resistance

Figure 1 shows the carrier activation ratio, defined as the sheet carrier concentration divided by implantation dose, of samples implanted using As or BF<sub>2</sub> with the ion energy ranging from 10 to 30 keV. The implanted doses were  $1 \times 10^{14}$  or  $5 \times 10^{14} \text{ cm}^{-2}$ . Post-implantation annealing was carried out at 950 °C for 10 seconds (RTA) or at 800 °C for 10 minutes (FA). The carrier activation ratio of the RTA samples was higher than that of the FA samples in all cases. In particular,

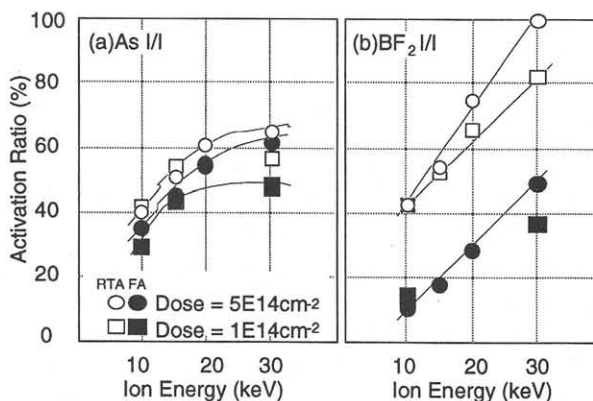


Fig. 1 Dependence of carrier activation ratio on the ion energy. (a) As ion implantation, (b) BF<sub>2</sub> ion implantation

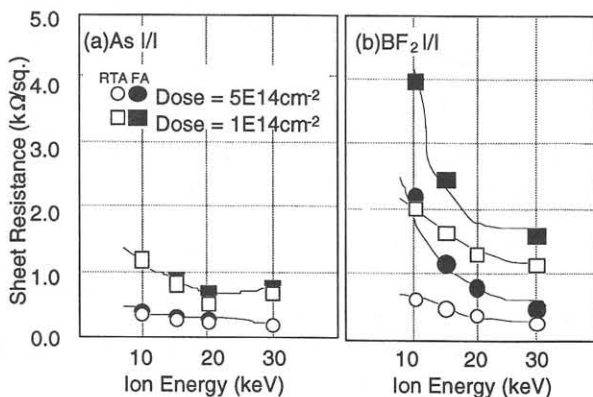


Fig. 2 Dependence of sheet resistance on the ion energy. (a) As ion implantation, (b) BF<sub>2</sub> ion implantation

RTA is essential for 10-keV BF<sub>2</sub> implantation to obtain low

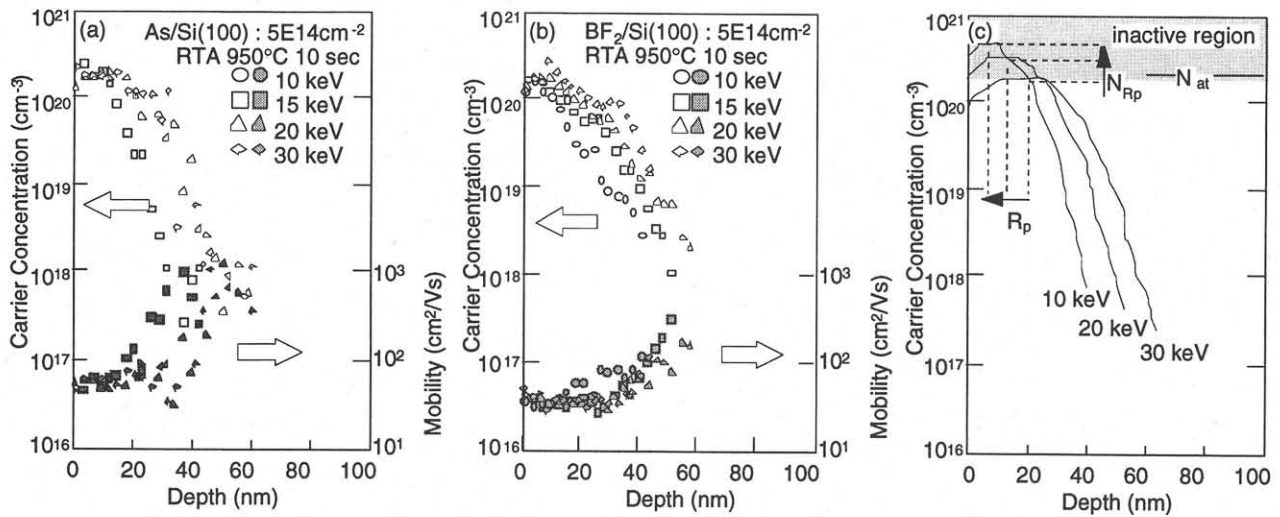


Fig. 3 Depth profiles of carriers and mobility.  
 (a) As ion implantation, (b)  $\text{BF}_2$  ion implantation,  
 (c) Model of energy dependence of carrier activation

sheet resistance (Fig. 2), because the recrystallization seemed to be imperfect when FA was used. In the case of 30-keV  $\text{BF}_2$  implantation, impurities were fully activated after RTA. On the other hand, the activation ratio was only 40% with the 10 keV implantation of both  $\text{BF}_2$  and As.

To clarify the cause of the lower activation in the case of 10-keV implantation, carrier profiles were obtained by stripping Hall measurement. Figure 3 shows the carrier and mobility profiles of the As or  $\text{BF}_2$  implanted samples at a dose of  $5 \times 10^{14} \text{ cm}^{-2}$  after RTA. The junction depth ( $x_j$ ) became shallower as the ion energy decreased. When the ion energy is decreased, the projection range ( $R_p$ ) is expected to be closer to the surface and the peak carrier concentration ( $N_{Rp}$ ) becomes higher as illustrated in Fig. 3(c). However, the peak carrier concentration is observed to be almost the same at about  $2 \times 10^{20} \text{ cm}^{-3}$  for  $\text{BF}_2$  and  $3 \times 10^{20} \text{ cm}^{-3}$  for As. This is because the implanted impurities at concentrations these levels are not activated.

Thus, the implantation dose must be optimized to obtain ultra-shallow diffused layers with low resistance. A dose above  $3 \times 10^{14} \text{ cm}^{-2}$  is essential when the ion energy is lowered to less than 10 keV, and with a dose of  $5 \times 10^{14} \text{ cm}^{-2}$ , we have obtained sufficiently low sheet resistance of 0.7  $\text{k}\Omega/\text{sq.}$  for  $\text{BF}_2$  and 0.4  $\text{k}\Omega/\text{sq.}$  for As.

### III. n-MOSFET Fabrication Process

To suppress the short-channel effect and to reduce  $V_{th}$  for low-power operation, B ions were implanted as a punchthrough stopper, and As ions as counter-doping. Then, a 4-nm-thick gate oxide and a P-doped poly-Si gate were formed. E-beam lithography was used to fabricate the gate electrode. After gate formation, low-energy As implantation was performed. This was followed by deep As ion implantation, then RTA was used to activate implanted impurity.

### IV. Parasitic Resistance of 0.15- $\mu\text{m}$ n-MOSFETs

We used the Chern method<sup>(3)</sup> to estimate the total S/D parasitic resistance of the n-MOSFETs. The fabricated devices are listed in Table 1. The S/D ultra-shallow diffused layers were formed by As implantation with an ion energy ranging from 10 to 20 keV (implanted doses either  $1 \times 10^{14}$  or

Table 1 Fabricated n-MOSFET samples

No.	implantation.	RTA	Rsd( $\Omega$ )	ps( $\Omega/\text{sq.}$ )	plot
#1	10 keV, $1\text{E}14 \text{ cm}^{-2}$	950°C 10 s	106.9	1.27 k	none
#2	10 keV, $5\text{E}14 \text{ cm}^{-2}$	950°C 10 s	59.6	0.34 k	▲
#3	15 keV, $1\text{E}14 \text{ cm}^{-2}$	950°C 10 s	78.4	0.84 k	none
#4	15 keV, $5\text{E}14 \text{ cm}^{-2}$	950°C 10 s	53.0	0.29 k	□
#5	20 keV, $1\text{E}14 \text{ cm}^{-2}$	950°C 10 s	61.8	0.56 k	none
#6	20 keV, $5\text{E}14 \text{ cm}^{-2}$	950°C 10 s	40.2	0.25 k	○

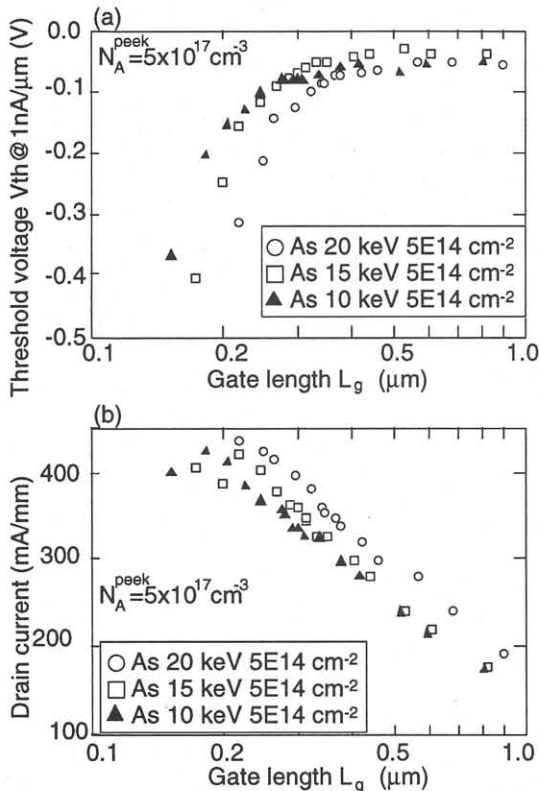


Fig. 4 Gate length ( $L_g$ ) dependence of n-MOSFET characteristics  
(a)  $V_{th}$  vs  $L_g$ , (b)  $I_d$  vs  $L_g$

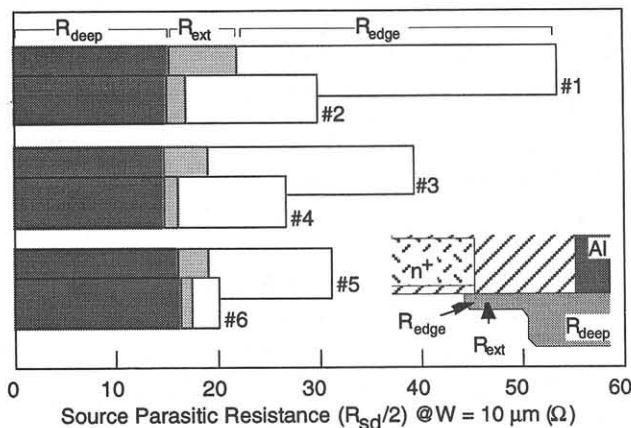


Fig. 5 Source parasitic resistance ( $R_{sd}/2$ ) as a function of ion energy. RTA was carried out at 950°C for 10 s.

$5 \times 10^{14} \text{ cm}^{-2}$ ). The dependence of threshold voltage ( $V_{th}$ ) and drain current ( $I_d$ ) on the gate length ( $L_g$ ) are shown in Fig. 4. The n-MOSFET fabricated using 10 keV As implantation shows better short-channel characteristics due to its shallower junction. However, it has a lower  $I_d$ . The S/D parasitic resistance ( $R_{sd}$ ) is also shown in Table 1. The  $R_{sd}$  consists of

the resistance of the ultra-shallow diffused layer ( $R_{ext}$ ), the deep-diffused layer including the contact resistance ( $R_{deep}$ ), and the edge resistance due to current crowding<sup>(4)</sup> ( $R_{edge}$ ). As the ion energy was decreased, source resistance ( $= R_{sd}/2$ ) increased as shown in Fig. 5, and this increase was larger when the implanted dose was  $1 \times 10^{14} \text{ cm}^{-2}$ . Since  $R_{deep}$  and the sheet resistance of the shallow diffused layer are almost constant, this increase is due to the increased S/D edge resistance. This observation contradicts the prediction that a shallow, abrupt diffused layer has smaller edge resistance<sup>(4)</sup>. Therefore, knowledge about two-dimensional dopant profiles is becoming more and more important in the fabrication of high-performance MOSFETs with gate length of less than  $0.15 \mu\text{m}$ .

## VI. Conclusion

In low-energy ion implantation for S/D formation in  $0.15\text{-}\mu\text{m}$  MOSFETs, degradation of the carrier activation and an increase in S/D edge resistance were found for the first time. These phenomena should be considered when using low-energy ion implantation to fabricate high-performance  $0.15\text{-}\mu\text{m}$  MOSFETs.

## Acknowledgments

We thank the members of the Process Integration Center of the Central Research Laboratory, Hitachi, Ltd., for the device fabrication.

## References

- (1) Byung G. Park, et al., IEEE Electron Device Lett. **13**(1992)507
- (2) M. C. Ozturk, et al., Appl. Phys. Lett. **52**(1988)963
- (3) J. G. J. Chern et al., IEEE Electron Device Lett., **EDL-1**(1980)170
- (4) K. K. Ng et al., IEEE Trans. Electron Device, **ED-33**(1986)965